PERGAMON

International Journal of Solids and Structures 36 (1999) 5507–5527

INTERNATIONAL JOURNAL OF SOLIDS and STRUCTURES

www.elsevier.com/locate/ijsolstr

Detection of finite mechanisms in symmetric structures

R.D. Kangwai, S.D. Guest*

Department of Engineering, University of Cambridge, Trumpington Street, Cambridge, CB2 1PZ, U.K.

Received 19 August 1997; in revised form 6 July 1998

Abstract

Using group representation theory, it is possible to block-diagonalise the equilibrium matrix of a symmetric structure. This analysis can identify the symmetry properties of any states of self-stress or mechanisms present in the structure. This paper will show that in some cases, this linear analysis, combined with symmetry arguments, can show that particular mechanisms of a symmetric structure must be finite.

1. Introduction

This paper will show how an analysis based on symmetry can provide considerable insight into the nature of symmetric structures which are both statically and kinematically indeterminate. In particular, it will show that in some cases a symmetry analysis can identify when such a structure admits a finite mechanism.

Previously, a number of authors have applied group representation theory to the analysis of symmetric structures, essentially to show how the efficiency of a computational analysis could be improved by block-diagonalising a stiffness matrix. In a forthcoming paper (Kangwai and Guest, 1999), we apply group representation theory to block-diagonalise the equilibrium matrix of a symmetric structure, and show that this provides useful insight into the structural response of such structures. In particular, it provides a useful classification of any states of self-stress or inextensional mechanisms present.

Using the same techniques as Kangwai and Guest (1999), this paper takes an additional step to investigate statically and kinematically indeterminate symmetric structures that admit finite mechanisms. An analysis is carried out on a ring structure originally investigated by Tarnai (1980) which belongs to a class of structures that satisfy Maxwell's rule, but is both statically and

* Corresponding author. Tel.: +44 01223 332721; fax: +44-1223 332662; e-mail: sdg@eng.cam.ac.uk

0020-7683/99/$ - see front matter
PII: S0020-7683(98)00234-0

kinematically indeterminate. Using symmetry arguments, the linear analysis represented by the equilibrium matrix will show that this ring structure contains a finite mechanism. This paper will also consider in general when such an analysis is valid.

The layout of this paper is as follows. The rest of this section gives some background on equilibrium and compatibility matrices, and also statically and kinematically indeterminate structures. Section 2 analyses a hexagonal ring with rotational and reflection symmetry properties, to show that it admits a finite mechanism. Section 3 analyses the same hexagonal ring at another configuration where there exists a kinematic bifurcation with four possible kinematic paths, of which only one can be identified using symmetry arguments. Finally, Section 4 concludes by discussing in general when a symmetry analysis can identify finite mechanisms.

1.1. Equilibrium, compatibility and flexibility matrices

Structural analysis requires three principles to be satisfied; that internal forces are in equilibrium with the applied load, that any internal deformation is compatible with external displacements, and that internal forces and displacements are related by a material law.

For small perturbations around the initial configuration of a structure, these relationships can be linearised as three matrix relationships. The system of static equilibrium equations for a structure is given by:

$$\mathbf{Hf} = \mathbf{p} \tag{1}$$

where $\mathbf{H}$ is the equilibrium matrix, $\mathbf{f}$ is the internal force vector and $\mathbf{p}$ is the external load vector. The system of kinematic compatibility equations is given by:

$$\mathbf{Cd} = \mathbf{e} \tag{2}$$

where $\mathbf{C}$ is the compatibility matrix, $\mathbf{d}$ is the external displacement vector and $\mathbf{e}$ is the internal deformation vector. The stress-strain relationship is given by:

$$\mathbf{Rf} = \mathbf{e} \tag{3}$$

where $\mathbf{R}$ is the flexibility matrix.

It can easily be shown by a virtual work argument that $\mathbf{C} = \mathbf{H}^{\mathrm{T}}$ (McGuire and Gallagher, 1979), and so the statics and kinematics of a structure are intimately bound together.

1.2. Statically and kinematically indeterminate structures

A statically determinate structure is a structure where the internal forces in equilibrium with any applied load can be uniquely determined, and this implies that it does not admit a state of self-stress. Similarly, a kinematically determinate structure is a structure where a linear analysis will find a unique configuration for any internal deformations, and this implies that there is no mechanism. Maxwell's rule is a well known formula which provides a necessary condition for both static and kinematic determinacy to occur together. For a 3-dimensional pin-jointed structure rigidly connected to a foundation, Maxwell's rule states:

$$b = 3j \tag{4}$$

where b is the total number of bars and j is the number of non-foundation joints. In this case, the equilibrium matrix of a structure is square.

However, Maxwell (1864) anticipated exceptions to his rule and these special cases have been investigated by a number of authors. These special cases include structures which satisfy Maxwell's rule but are both statically and kinematically indeterminate and hence contain states of self-stress, and either infinitesimal or finite mechanisms (Mohr, 1885; Föppl, 1912; Tarnai, 1980). A finite mechanism will allow the joints to move freely for a finite distance without any change in bar-lengths, while an infinitesimal mechanism will cause second-order or higher changes in bar-lengths when the joints move.

Tarnai (1980) pointed out that the topological condition expressed by Maxwell's rule is not sufficient to determine whether a structure is stiff or not. The stiffness can only be determined by the geometry of the structure. A more complete analysis of the equilibrium and compatibility matrices is required to provide the following expressions:

$$\begin{aligned} s &= b-r \\ m &= 3J-r \end{aligned} \tag{5}$$

where r is the rank of either the equilibrium matrix or its transpose, the compatibility matrix, s is the degree of static indeterminacy and m is the degree of kinematic indeterminacy.

Structures that have too few constraints to satisfy Maxwell's rule will usually have kinematic mobility, as the analysis will not admit a unique solution, and hence finite mechanisms will exist. However, a number of authors have previously studied the particular case where these structures do have first-order stiffness (Kötter, 1912; Fuller, 1975; Calladine, 1978; Pellegrino and Calladine, 1986; 1991; Kuznetsov, 1988; 1991). This class of structure is now commonly referred to as tensegrity structures. In these structures the equilibrium and compatibility matrices must be rank deficient. The interaction between the resultant state of self-stress and any mechanisms is then crucial to understanding the behaviour of the structure—it can be considered that a state of self-stress stiffens any mechanisms of the structure. Care must be taken, however, as in some apparently similar structures, the state of self-stress is unstable, and can provide no stiffening effect (Kuznetsov, 1988; 1991; Pellegrino and Calladine, 1991).

This paper examines a very different type of structure that satisfies Maxwell's rule, and yet allows finite mechanisms. There are, of course, trivial examples of this where physically distinct parts of the structure may admit a state of self-stress, or a mechanism; an example is shown in Fig. 1. Mobilising the mechanism in the lower half of this structure will have no effect on the state of self-stress in the upper half; the structure will remain both statically and kinematically indeterminate—the mechanism is obviously finite.

This paper will concentrate not on the trivial case represented by Fig. 1, but on a related type of structure where states of self-stress and mechanisms are symmetrically distinct. The existence of a finite mechanism in these structures is then certainly not obvious. Baker, in an appendix to Tarnai (1989), has explored the possibility of symmetry explaining the apparent reduction in the number of constraints in symmetric ring structures. We will show that using symmetry arguments to block-diagonalise the equilibrium matrix of a structure can show when states of self-stress and mechanism are symmetrically distinct, hence explaining the existence of finite mechanisms in these structures.

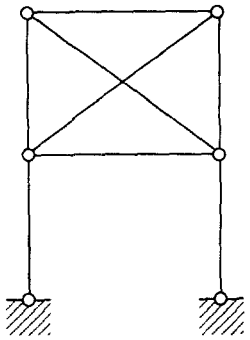

Fig. 1. Simple structure that satisfies Maxwell's rule but has a physically distinct finite mechanism and state of self-stress. The two diagonal bars are not connected and are free to move adjacent to one another.

2. Hexagonal ring with rotation and reflection symmetry

In Section 1.2., we mentioned the existence of special cases which form exceptions to Maxwell's rule. In this section we will analyse one of these special cases, a structure which satisfies Maxwell's rule but in fact has a finite mechanism.

Tarnai (1980) investigated the structural rigidity of a class of pin-jointed reticulated cylinder structures. These reticulated cylinders consist of congruent rings with n-fold rotational symmetry, and are connected to a rigid foundation; two examples are shown in Fig. 2. Tarnai showed that while keeping the same topological properties, the state of static and kinematic determinacy of these reticulated cylinders is dependent on the geometry of the structure. The cylinder shown in Fig. 2(a) satisfies Maxwell's rule and is indeed both statically and kinematically determinate.

However, for a cylinder with the same topological properties but which also has n planes of reflection symmetry, the static and kinematic determinacy of the cylinder is dependent on n; an example for $n = 6$ is shown in Fig. 2(b). If n is odd, the cylinder is statically and kinematically determinate. If n is even, the cylinder is statically and kinematically indeterminate and the degree of indeterminacy is always one, irrespective of the number of rings in the cylinder. Tarnai showed that the single state of self-stress always occurs in the lowest ring, while the inextensional mechanism always occurs in the uppermost ring, and is indeed a finite mechanism. The distinct difference in behaviour between these structures when n is even or odd is very clear for even a simple card model.

In this section, the analysis is limited to a single hexagonal ring with 6-fold rotational symmetry and 6 planes of reflection symmetry, shown in Fig. 3. The hexagonal ring consists of $b = 18$ bar-elements and $j = 6$ pin-joints. Maxwell's rule for a pin-jointed structure connected to a foundation, gives $3j - b = 0$ and hence the hexagonal ring would appear to be both statically and kinematically determinate. However, standard structural analysis shows that the (18×18) equilibrium matrix $\mathbf{H}$ has rank 17, that is the hexagonal ring contains $s = 1$ state of self-stress and $m = 1$ inextensional mechanism.

This section describes how the application of group representation theory to the symmetry properties of the hexagonal ring can be used to find symmetry-adapted coordinate systems for the load and bar-force vector spaces. These symmetry-adapted coordinate systems are made up of

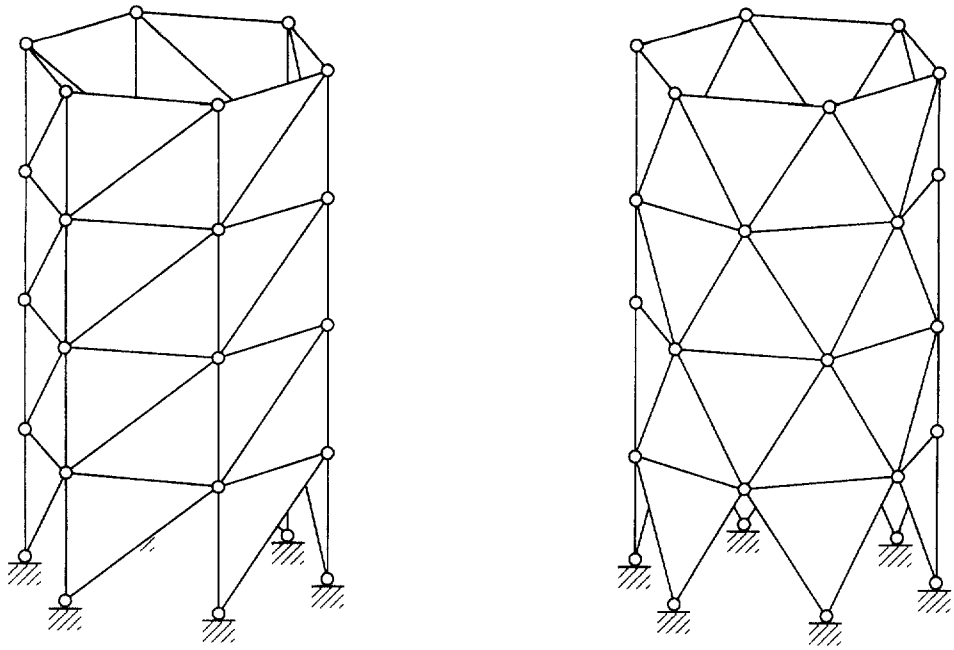

Fig. 2. Reticulated cylinders with $\mathbf{C}_{6v}$ symmetry.

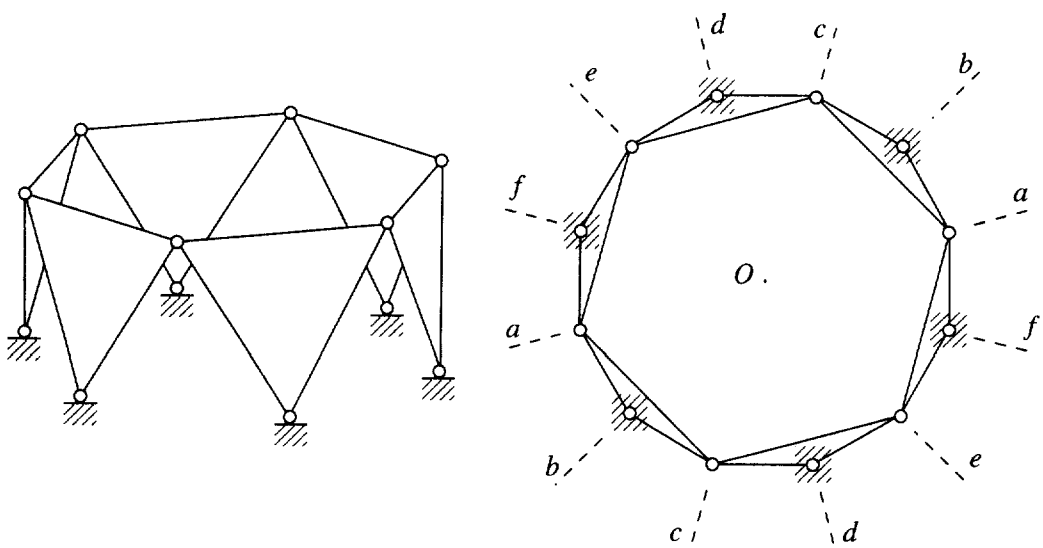

Fig. 3. Hexagonal ring with $\mathbf{C}_{6v}$ symmetry.

vector symmetry subspaces, each of which have particular symmetry properties of the hexagonal ring. We then show how these symmetry-adapted coordinate systems are used to block-diagonalise the equilibrium matrix $\mathbf{H}$ of the hexagonal ring, into symmetry-adapted equilibrium submatrix blocks $\mathbf{H}^{(\mu)i}$, which considerably simplifies the analysis of the structure and gives valuable insight into the nature of the finite mechanism.

We will only present the symmetry-adapted coordinate systems for the hexagonal ring and not explain how they may be found. For a more comprehensive description of group representation theory applied to symmetric structures, see the papers, Kangwai et al. (1999) and Kangwai and Guest (1999).

2.1. Symmetry-adapted coordinate systems

The hexagonal ring is a structure that, when acted on by particular symmetry operations, is left in a geometrically and mechanically unaltered configuration, i.e., an equivalent configuration. The hexagonal ring is transformed into an equivalent configuration by the following set of symmetry operations:

(1) The identity, symmetry operation E.
(2) Rotation by 60° about the origin O, symmetry operation C_6.
(3) Rotation by 120° about the origin O, symmetry operation C_6^2.
(4) Rotation by 180° about the origin O, symmetry operation C_6^3.
(5) Rotation by 240° about the origin O, symmetry operation C_6^4.
(6) Rotation by 300° about the origin O, symmetry operation C_6^5.
(7) Reflection in the vertical plane a, symmetry operation σ_a.
(8) Reflection in the vertical plane b, symmetry operation σ_b.
(9) Reflection in the vertical plane c, symmetry operation σ_c.
(10) Reflection in the vertical plane d, symmetry operation σ_d.
(11) Reflection in the vertical plane e, symmetry operation σ_e.
(12) Reflection in the vertical plane f, symmetry operation σ_f.

These twelve operations $\{E, C_6, C_6^2, C_6^3, C_6^4, C_6^5, \sigma_a, \sigma_b, \sigma_c, \sigma_d, \sigma_e, \sigma_f\}$ constitute a *symmetry group* $\mathbf{C}_{6v}$.

There are a limited number of symmetry groups, and associated with each symmetry group are a set of *irreducible matrix representations*. The six irreducible representations $\Gamma^{(A_1)}$ to $\Gamma^{(E_2)}$ of a symmetry group $\mathbf{C}_{6v}$ are shown in Table 1. Each of these irreducible representations represents a fundamental aspect of the symmetry of the structure. We show in Kangwai and Guest (1999) how we could make use of the irreducible representations fo find symmetry-adapted coordinate systems for both the internal vector space $\mathbb{V}_\mathbf{p}$ (e.g., a space suitable for expressing bar-forces and extensions) and the external vector space $\mathbb{V}_\mathbf{f}$ (e.g., a space suitable for expressing loads and displacements).

The symmetry-adapted coordinate systems split the vector spaces into a number of symmetry subspaces $\mathbb{V}_\mathbf{p}^{(\mu)i}$ and $\mathbb{V}_\mathbf{f}^{(\mu)i}$, each corresponding to a row i of the irreducible representation μ, and each having different symmetry properties. For symmetry group $\mathbf{C}_{6v}$ there are eight symmetry subspaces for the internal and external vector spaces, and their symmetry properties are given below.

Table 1
Irreducible representations of symmetry group $\mathbf{C}_{6v}$

$\mathbf{C}_{6v}$	E	C_6	C_6^2	C_6^3	C_6^4	C_6^5
$\Gamma^{(A_1)}$	1	1	1	1	1	1
$\Gamma^{(A_2)}$	1	1	1	1	1	1
$\Gamma^{(B_1)}$	1	−1	1	−1	1	−1
$\Gamma^{(B_2)}$	1	−1	1	−1	1	−1
$\Gamma^{(E_1)}$	$\begin{bmatrix}1 & 0\\ 0 & 1\end{bmatrix}$	$\begin{bmatrix}1/2 & -\sqrt{3}/2\\ \sqrt{3}/2 & 1/2\end{bmatrix}$	$\begin{bmatrix}-1/2 & -\sqrt{3}/2\\ \sqrt{3}/2 & -1/2\end{bmatrix}$	$\begin{bmatrix}-1 & 0\\ 0 & -1\end{bmatrix}$	$\begin{bmatrix}-1/2 & \sqrt{3}/2\\ -\sqrt{3}/2 & -1/2\end{bmatrix}$	$\begin{bmatrix}1/2 & \sqrt{3}/2\\ -\sqrt{3}/2 & 1/2\end{bmatrix}$
$\Gamma^{(E_2)}$	$\begin{bmatrix}1 & 0\\ 0 & 1\end{bmatrix}$	$\begin{bmatrix}-1/2 & -\sqrt{3}/2\\ \sqrt{3}/2 & -1/2\end{bmatrix}$	$\begin{bmatrix}-1/2 & \sqrt{3}/2\\ -\sqrt{3}/2 & -1/2\end{bmatrix}$	$\begin{bmatrix}1 & 0\\ 0 & 1\end{bmatrix}$	$\begin{bmatrix}-1/2 & -\sqrt{3}/2\\ \sqrt{3}/2 & -1/2\end{bmatrix}$	$\begin{bmatrix}-1/2 & -\sqrt{3}/2\\ -\sqrt{3}/2 & -1/2\end{bmatrix}$

σ_a	σ_b	σ_c	σ_d	σ_e	σ_f
1	1	1	1	1	1
−1	−1	−1	−1	−1	−1
1	−1	1	−1	1	−1
−1	1	−1	1	−1	1
$\begin{bmatrix}1 & 0\\ 0 & -1\end{bmatrix}$	$\begin{bmatrix}1/2 & \sqrt{3}/2\\ \sqrt{3}/2 & -1/2\end{bmatrix}$	$\begin{bmatrix}-1/2 & \sqrt{3}/2\\ \sqrt{3}/2 & 1/2\end{bmatrix}$	$\begin{bmatrix}-1 & 0\\ 0 & 1\end{bmatrix}$	$\begin{bmatrix}-1/2 & -\sqrt{3}/2\\ -\sqrt{3}/2 & 1/2\end{bmatrix}$	$\begin{bmatrix}1/2 & -\sqrt{3}/2\\ -\sqrt{3}/2 & -1/2\end{bmatrix}$
$\begin{bmatrix}1 & 0\\ 0 & -1\end{bmatrix}$	$\begin{bmatrix}-1/2 & \sqrt{3}/2\\ \sqrt{3}/2 & 1/2\end{bmatrix}$	$\begin{bmatrix}-1/2 & -\sqrt{3}/2\\ -\sqrt{3}/2 & 1/2\end{bmatrix}$	$\begin{bmatrix}1 & 0\\ 0 & -1\end{bmatrix}$	$\begin{bmatrix}-1/2 & \sqrt{3}/2\\ \sqrt{3}/2 & 1/2\end{bmatrix}$	$\begin{bmatrix}-1/2 & -\sqrt{3}/2\\ -\sqrt{3}/2 & 1/2\end{bmatrix}$

(1) $\mathbb{V}_{\mathbf{p}}^{(A_1)}$ and $\mathbb{V}_{\mathbf{f}}^{(A_1)}$: the full symmetry group $\mathbf{C}_{6v}$.
(2) $\mathbb{V}_{\mathbf{p}}^{(A_2)}$ and $\mathbb{V}_{\mathbf{f}}^{(A_2)}$: 6-fold rotational symmetry, symmetry group $\mathbf{C}_6$.
(3) $\mathbb{V}_{\mathbf{p}}^{(B_1)}$ and $\mathbb{V}_{\mathbf{f}}^{(B_1)}$: 3-fold rotational symmetry and reflection symmetry in planes a, c and e, symmetry group $\mathbf{C}_{3v}$.
(4) $\mathbb{V}_{\mathbf{p}}^{(B_2)}$ and $\mathbb{V}_{\mathbf{f}}^{(B_2)}$: 3-fold rotational symmetry and reflection symmetry in planes b, d and f, symmetry group $\mathbf{C}_{3v}$.
(5) $\mathbb{V}_{\mathbf{p}}^{(E_1)1}$ and $\mathbb{V}_{\mathbf{f}}^{(E_1)1}$: reflection symmetry in plane a, symmetry group $\mathbf{C}_s$.
(6) $\mathbb{V}_{\mathbf{p}}^{(E_1)2}$ and $\mathbb{V}_{\mathbf{f}}^{(E_1)2}$: reflection symmetry in plane d, symmetry group $\mathbf{C}_s$.
(7) $\mathbb{V}_{\mathbf{p}}^{(E_2)1}$ and $\mathbb{V}_{\mathbf{f}}^{(E_2)1}$: 2-fold rotational symmetry and reflection symmetry in planes a and d, symmetry group $\mathbf{C}_{2v}$.
(8) $\mathbb{V}_{\mathbf{p}}^{(E_2)2}$ and $\mathbb{V}_{\mathbf{f}}^{(E_2)2}$: 2-fold rotational symmetry, symmetry group $\mathbf{C}_2$.

These symmetry properties are defined by the symmetry group and are independent of the topology of the structure in question. However, we show in Kangwai and Guest (1999) how it is possible to find basis vectors for each of the symmetry subspaces $\mathbb{V}_{\mathbf{p}}^{(\mu)i}$. These basic vectors can then be written as columns of a matrix $\mathbf{V}_{\mathbf{p}}^{(\mu)i}$. Group representation theory shows that together, these basis vectors span the whole space $\mathbb{V}_{\mathbf{p}}$. Hence it is possible to write an orthogonal matrix $\mathbf{V}_{\mathbf{p}}$ which transforms

load vectors between the original and the symmetry-adapted coordinate system. For symmetry group $\mathbf{C}_{6v}$ this matrix is:

$$\mathbf{V}_\mathbf{p} = \left(\mathbf{V}_\mathbf{p}^{(A_1)} | \mathbf{V}_\mathbf{p}^{(A_2)} | \mathbf{V}_\mathbf{p}^{(B_1)} | \mathbf{V}_\mathbf{p}^{(B_2)} | \mathbf{V}_\mathbf{p}^{(E_1)1} | \mathbf{V}_\mathbf{p}^{(E_1)2} | \mathbf{V}_\mathbf{p}^{(E_2)1} | \mathbf{V}_\mathbf{p}^{(E_2)2} \right) \tag{6}$$

Similarly, the orthogonal matrix $\mathbf{V}_\mathbf{f}$ which transforms bar-force vectors between the original and the symmetry-adapted coordinate system:

$$\mathbf{V}_\mathbf{f} = \left(\mathbf{V}_\mathbf{f}^{(A_1)} | \mathbf{V}_\mathbf{f}^{(A_2)} | \mathbf{V}_\mathbf{f}^{(B_1)} | \mathbf{V}_\mathbf{f}^{(B_2)} | \mathbf{V}_\mathbf{f}^{(E_1)1} | \mathbf{V}_\mathbf{f}^{(E_1)2} | \mathbf{V}_\mathbf{f}^{(E_2)1} | \mathbf{V}_\mathbf{f}^{(E_2)2} \right) \tag{7}$$

Figures 4 and 5 show a set of basis vectors for the first four internal and external symmetry subspaces of our example structure. The basis vectors for the remaining symmetry subspaces have not been shown in the interests of brevity, and also because they do not participate in the later discussion of the properties of the structure.

2.2. *Block-diagonalisation of the equilibrium matrix with C_{6v} symmetry*

External loads applied to a structure, which have a particular type of symmetry, will be in equilibrium with internal forces which also have the same symmetry. Therefore, using symmetry-adapted coordinate systems will block-diagonalise the equilibrium matrix.

Consider starting with the system of equilibrium relationships between the internal bar-forces $\mathbf{f}$ and the external loads $\mathbf{p}$, written in some general coordinate system:

$$\mathbf{H}\mathbf{f} = \mathbf{p} \tag{8}$$

By writing the load and bar-force vectors in their symmetry-adapted coordinate systems (a $\sim$ is used for the symmetry-adapted systems):

$$\tilde{\mathbf{f}} = \mathbf{V}_\mathbf{f}^\mathrm{T}\mathbf{f} \tag{9}$$

$$\tilde{\mathbf{p}} = \mathbf{V}_\mathbf{p}^\mathrm{T}\mathbf{p} \tag{10}$$

and substituting Eqns 9 and 10 into the equilibrium equation $\mathbf{Hf} = \mathbf{p}$ gives:

$$\mathbf{H}\mathbf{V}_\mathbf{f}\tilde{\mathbf{f}} = \mathbf{V}_\mathbf{p}\tilde{\mathbf{p}} \tag{11}$$

Hence, the symmetry-adapted equilibrium relationship is now:

$$\tilde{\mathbf{H}}\tilde{\mathbf{f}} = \tilde{\mathbf{p}} \tag{12}$$

where $\tilde{\mathbf{H}}$ is the block-diagonalised equilibrium matrix:

$$\tilde{\mathbf{H}} = \mathbf{V}_\mathbf{p}^\mathrm{T}\mathbf{H}\mathbf{V}_\mathbf{p} \tag{13}$$

For the hexagonal ring shown in Fig. 3, the block-diagonalised equilibrium matrix $\tilde{\mathbf{H}}$ has the form shown in Eqn 14 below. Each of the equilibrium blocks have full rank.

Each of the equilibrium blocks $\tilde{\mathbf{H}}^{(\mu)i}$, operates on symmetry-adapted load and bar-force vectors $\tilde{\mathbf{p}}^{(\mu)i}$ and $\tilde{\mathbf{f}}^{(\mu)i}$ in the corresponding symmetry subspaces $\mathbb{V}_\mathbf{p}^{(\mu)i}$ and $\mathbb{V}_\mathbf{f}^{(\mu)i}$. Hence, the original equi-

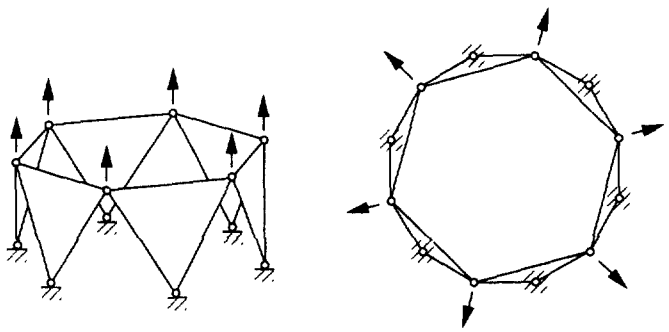

(a) 2-dimensional symmetry subspace $\mathbb{V}_{\mathbf{p}}^{(A_1)}$

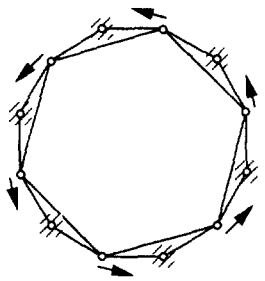

(b) 1-dimensional symmetry subspace $\mathbb{V}_{\mathbf{p}}^{(A_2)}$

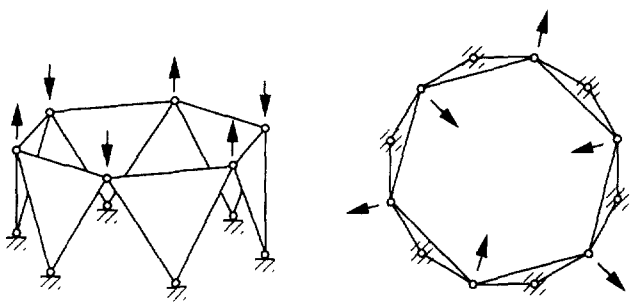

(c) 2-dimensional symmetry subspace $\mathbb{V}_{\mathbf{p}}^{(B_1)}$

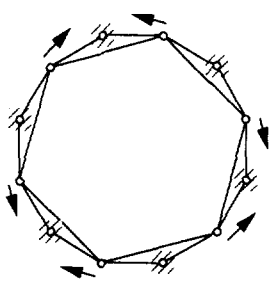

(d) 1-dimensional symmetry subspace $\mathbb{V}_{\mathbf{p}}^{(B_2)}$

Fig. 4. External symmetry subspaces $\mathbb{V}_{\mathbf{p}}^{(A_1)}$, $\mathbb{V}_{\mathbf{p}}^{(A_2)}$, $\mathbb{V}_{\mathbf{p}}^{(B_1)}$ and $\mathbb{V}_{\mathbf{p}}^{(B_2)}$. Each arrow is of magnitude $1/\sqrt{6}$, to give resultant basis vectors of unit length.

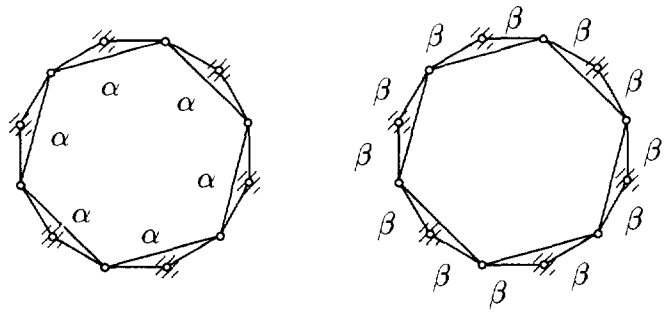

(a) 2-dimensional symmetry subspace $\mathbb{V}_{\mathbf{f}}^{(A_1)}$

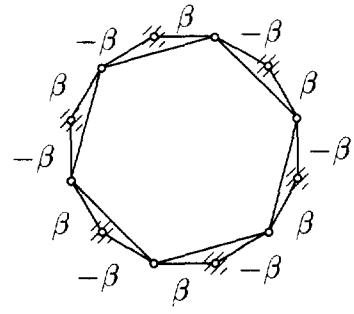

(b) 1-dimensional symmetry subspace $\mathbb{V}_{\mathbf{f}}^{(A_2)}$

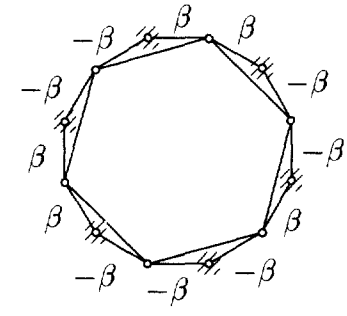

(c) 1-dimensional symmetry subspace $\mathbb{V}_{\mathbf{f}}^{(B_1)}$

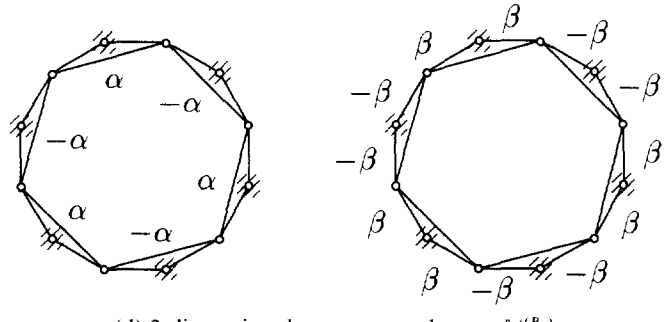

(d) 2-dimensional symmetry subspace $\mathbb{V}_{\mathbf{p}}^{(B_2)}$

Fig. 5. Internal symmetry subspaces $\mathbb{V}_{\mathbf{f}}^{(A_1)}$, $\mathbb{V}_{\mathbf{f}}^{(A_2)}$, $\mathbb{V}_{\mathbf{f}}^{(B_1)}$ and $\mathbb{V}_{\mathbf{f}}^{(B_2)}$. α and β refer to the magnitude of the force or extension in the corresponding bar. $\alpha = 1/\sqrt{6}$ and $\beta = 1/\sqrt{12}$ give resultant basis vectors of unit length.

$$\tilde{\mathbf{H}} = \begin{bmatrix} \tilde{\mathbf{H}}^{(A_1)}\,(2\times 2) & & & & & & \\ & \tilde{\mathbf{H}}^{(A_2)}\,(1\times 1) & & & & & \\ & & \tilde{\mathbf{H}}^{(B_1)}\,(2\times 1) & & & & \\ & & & \tilde{\mathbf{H}}^{(B_2)}\,(1\times 2) & & & \\ & & & & \tilde{\mathbf{H}}^{(E_1)1}\,(3\times 3) & & \\ & & & & & \tilde{\mathbf{H}}^{(E_1)2}\,(3\times 3) & \\ & & & & & & \tilde{\mathbf{H}}^{(E_2)1}\,(3\times 3) \\ & & & & & & & \tilde{\mathbf{H}}^{(E_2)2}\,(3\times 3) \end{bmatrix} \tag{14}$$

librium equation $\mathbf{Hf} = \mathbf{p}$, has been decomposed into eight independent symmetry-adapted equilibrium subequations:

$$\tilde{\mathbf{H}}^{(\mu)i}\tilde{\mathbf{f}}^{(\mu)i} = \tilde{\mathbf{p}}^{(\mu)i} \tag{15}$$

where each $\tilde{\mathbf{H}}^{(\mu)i}$ gives the relationship between load and bar-force vectors that have particular symmetry properties, as described in Section 2.1.

Of particular interest are the first four equilibrium blocks along the diagonal, which we shall examine in more detail. Using the load and bar-force symmetry-adapted coordinate systems shown in Figs 4 and 5 respectively, these equilibrium blocks are:

$$\tilde{\mathbf{H}}^{(A_1)} = \begin{bmatrix} 0 & -1.2100 \\ 1 & 0.1895 \end{bmatrix}$$

$$\tilde{\mathbf{H}}^{(A_2)} = [-0.7071]$$

$$\tilde{\mathbf{H}}^{(B_1)} = \begin{bmatrix} -1.2100 \\ 0.1895 \end{bmatrix}$$

$$\tilde{\mathbf{H}}^{(B_2)} = [-1.7321 \quad -0.7071] \tag{16}$$

Thus, for example, -0.7071 times the internal bar-forces shown in Fig. 5(b), are in equilibrium with the external loads shown in Fig. 4(b).

In general, an equilibrium matrix $\mathbf{H}$ is a $(p \times q)$ matrix of rank r, and from the equilibrium matrix $\mathbf{H}$ it is possible to find the states of self-stress and the inextensional mechanisms of a structure (Pellegrino and Calladine, 1986). We can see that the block-diagonalised equilibrium matrix $\tilde{\mathbf{H}}$ also contains $(p^{(\mu)i} \times q^{(\mu)i})$ submatrix blocks of rank $r^{(\mu)i}$, and hence the analysis for states of self-stress and the inextensional mechanisms can be carried over to these independent equilibrium submatrix blocks $\tilde{\mathbf{H}}^{(\mu)i}$.

The block-diagonalised equilibrium matrix $\tilde{\mathbf{H}}$ consists of eight independent equilibrium submatrix blocks of which $\tilde{\mathbf{H}}^{(A_1)}$, $\tilde{\mathbf{H}}^{(A_2)}$, $\tilde{\mathbf{H}}^{(E_1)1}$, $\tilde{\mathbf{H}}^{(E_1)2}$, $\tilde{\mathbf{H}}^{(E_2)1}$ and $\tilde{\mathbf{H}}^{(E_2)2}$, are all square matrices of full rank, and hence do not contain any states of self-stress or inextensional mechanisms. The remaining two submatrix blocks, $\tilde{\mathbf{H}}^{(B_1)}$ and $\tilde{\mathbf{H}}^{(B_2)}$, are analysed below.

2.2.1. *Mechanism in the third equilibrium submatrix block*

$$\tilde{\mathbf{H}}^{(B_1)} = \begin{bmatrix} -1.2100 \\ 0.1895 \end{bmatrix}$$

The (2×1) equilibrium submatrix $\tilde{\mathbf{H}}^{(B_1)}$, corresponding to the irreducible matrix representation $\mathbf{\Gamma}^{(B_1)}$, is of rank 1 and hence will have a load vector in the corresponding load vector symmetry subspace $\mathbb{V}_{\mathbf{p}}^{(B_1)}$, which cannot be equilibrated. The inextensional mechanism induced by this load vector, is a displacement vector $\tilde{\mathbf{d}}_{\mathbf{m}}^{(B_1)}$, which is compatible with zero bar elongations, and as the compatibility matrix is the transpose of the equilibrium matrix, this can be written:

$$\tilde{\mathbf{C}}^{(B_1)}\tilde{\mathbf{d}}_{\mathbf{m}}^{(B_1)} = \tilde{\mathbf{H}}^{(B_1)\mathrm{T}}\tilde{\mathbf{d}}_{\mathbf{m}}^{(B_1)} = 0 \tag{17}$$

Thus, the mechanism is given by the nullspace of $\tilde{\mathbf{H}}^{(B_1)\mathrm{T}}$:

$$\tilde{\mathbf{d}}_{\mathbf{m}}^{(B_1)} = \begin{bmatrix} -0.1547 \\ -0.9880 \end{bmatrix} \tag{18}$$

Because the inextensional mechanism is from the third symmetry subspace $\mathbb{V}_{\mathbf{p}}^{(B_1)}$, it has $\mathbf{C}_{3v}$ symmetry properties, i.e., 3-fold rotational symmetry and reflection symmetry in planes a, c and e. The inextensional mechanism is shown in Fig. 6.

2.2.2. *State of self-stress in the fourth equilibrium submatrix block*

$$\tilde{\mathbf{H}}^{(B_2)} = [-1.7321 \quad -0.7071]$$

The (1×2) equilibrium submatrix $\tilde{\mathbf{H}}^{(B_2)}$, corresponding to the irreducible matrix representation $\mathbf{\Gamma}^{(B_2)}$ is rank 1, and hence will have a state of self-stress present in the corresponding bar-force vector symmetry subspace $\mathbb{V}_{\mathbf{f}}^{(B_2)}$. The state of self-stress is a bar-force vector $\tilde{\mathbf{f}}_{\mathbf{s}}^{(B_2)}$, in equilibrium with zero load vectors:

$$\tilde{\mathbf{H}}^{(B_2)}\tilde{\mathbf{f}}_{\mathbf{s}}^{(B_2)} = 0 \tag{19}$$

and is given by the nullspace of $\tilde{\mathbf{H}}^{(B_2)}$:

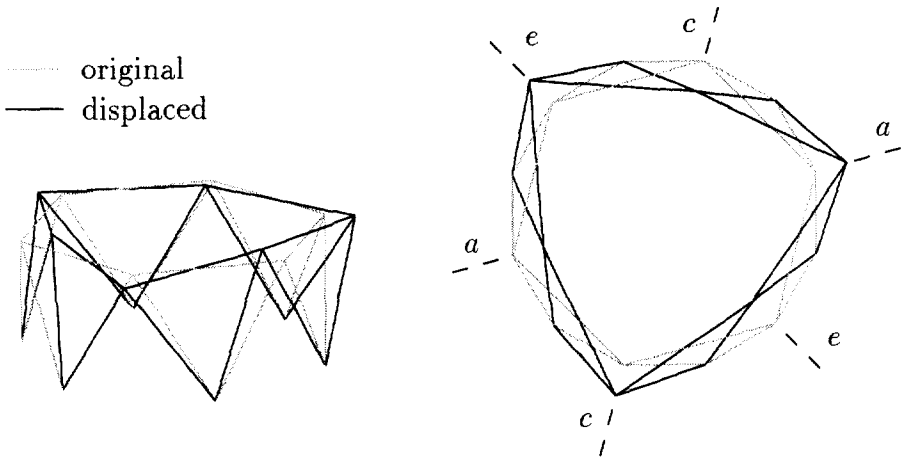

Fig. 6. Inextensional mechanism in symmetry subspace $\mathbb{V}_{\mathrm{p}}^{(B_1)}$.

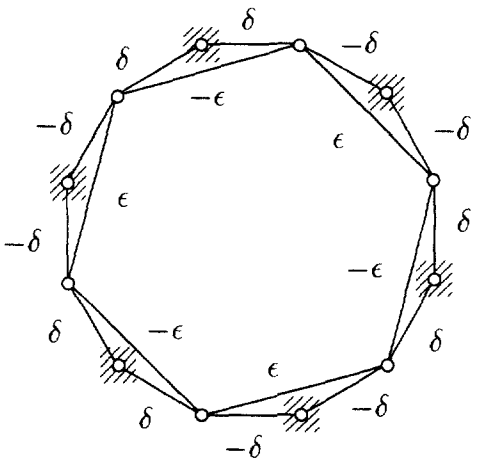

Fig. 7. State of self-stress in symmetry subspace $\mathbb{V}_{\mathrm{f}}^{(B_2)}$. $\delta = 1/\sqrt{14}$ and $\varepsilon = 1/\sqrt{42}$

$$\tilde{\mathbf{f}}_{\mathrm{s}}^{(B_2)} = \begin{bmatrix} -0.3780 \\ 0.9258 \end{bmatrix} \tag{20}$$

Because the state of self-stress is from the fourth symmetry subspace $\mathbb{V}_{\mathrm{f}}^{(B_2)}$, it also has $\mathbf{C}_{3v}$ symmetry properties, i.e., 3-fold rotational symmetry, but now reflection symmetry is in planes b, d and e. The state of self-stress is shown in Fig. 7.

2.3. Block diagonalisation of the equilibrium matrix with C_{3v} symmetry

The aim of our investigation is to determine whether the inextensional mechanism discovered in Section 2.2.1. is finite or infinitesimal. However, it is clear that the analysis we have carried out

will lose validity as soon as the mechanism is mobilised. The structure will lose its $\mathbf{C}_{6v}$ symmetry and instead will have only $\mathbf{C}_{3v}$ symmetry. Thus, to make further progress, it is necessary to reanalyse the structure using symmetry group $\mathbf{C}_{3v}$.

The following six symmetry operations constitute the symmetry group $\mathbf{C}_{3v}$:

(1) The identity, symmetry operation E.
(2) Rotation by 120° about the origin O, symmetry operation C_3.
(3) Rotation by 240° about the origin O, symmetry operation C_3^2.
(4) Reflection in the vertical plane a, symmetry operation σ_a.
(5) Reflection in the vertical plane c, symmetry operation σ_c.
(6) Reflection in the vertical plane e, symmetry operation σ_e.

For the hexagonal ring in its original configuration, both the load vector space $\mathbb{V}_\mathbf{p}$ and the bar-force vector space $\mathbb{V}_\mathbf{f}$ are now decomposed into four symmetry subspaces, defined by the irreducible representations of symmetry group $\mathbf{C}_{3v}$, shown in Table 2. The symmetry properties of the load and bar-force vector symmetry subspaces are given below.

(1) $\mathbb{V}_\mathbf{p}^{(A_1)}$ and $\mathbb{V}_\mathbf{f}^{(A_1)}$: the full symmetry of symmetry group $\mathbf{C}_{3v}$.
(2) $\mathbb{V}_\mathbf{p}^{(A_2)}$ and $\mathbb{V}_\mathbf{f}^{(A_2)}$: 3-fold rotational symmetry, symmetry group $\mathbf{C}_3$.
(3) $\mathbb{V}_\mathbf{p}^{(E_1)}$ and $\mathbb{V}_\mathbf{f}^{(E_1)}$: reflection symmetry in plane a, symmetry group $\mathbf{C}_s$.
(4) $\mathbb{V}_\mathbf{p}^{(E_2)}$ and $\mathbb{V}_\mathbf{f}^{(E_2)}$: reflection anti-symmetry in plane a, no symmetry.

Although it may now appear to be necessary to completely reanalyse the structure using symmetry group $\mathbf{C}_{3v}$, it is in fact possible to find the symmetry subspaces using a concept called *subduction*, or the *descent of symmetry*. Table 3 shows one way in which $\mathbf{C}_{6v}$ symmetry subspaces can combine to form the $\mathbf{C}_{3v}$ symmetry subspaces. This descent of symmetry is valid for any structure with $\mathbf{C}_{6v}$ symmetry, irrespective of its topology. Similar tables can be found for all symmetry groups, and a comprehensive study of symmetry groups and the relationships between the different groups is given by Altmann and Herzig (1994). Now it is only necessary to combine the $\mathbf{C}_{6v}$ symmetry subspaces according to the descent of symmetry shown in Table 3 in order to find the $\mathbf{C}_{3v}$ symmetry subspaces. For example, the vector basis $\mathbf{V}_\mathbf{p}^{(A_1)}$ is now given by the basis vectors in Figs 4(a) and (c). Using the load and bar-force vector symmetry-adapted coordinate systems with $\mathbf{C}_{3v}$ symmetry properties, the block-diagonalised equilibrium matrix $\tilde{\mathbf{H}}$ now has the form shown in Eqn. 14.

Table 2
Irreducible representations of symmetry group $\mathbf{C}_{3v}$

$\mathbf{C}_{3v}$	E	C_3	C_3^2	σ_a	σ_c	σ_e
$\Gamma^{(A_1)}$	1	1	1	1	1	1
$\Gamma^{(A_2)}$	1	1	1	−1	−1	−1
$\Gamma^{(E)}$	$\begin{bmatrix}1 & 0\\ 0 & 1\end{bmatrix}$	$\begin{bmatrix}-1/2 & -\sqrt{3}/2\\ \sqrt{3}/2 & -1/2\end{bmatrix}$	$\begin{bmatrix}-1/2 & \sqrt{3}/2\\ -\sqrt{3}/2 & -1/2\end{bmatrix}$	$\begin{bmatrix}1 & 0\\ 0 & -1\end{bmatrix}$	$\begin{bmatrix}-1/2 & \sqrt{3}/2\\ \sqrt{3}/2 & 1/2\end{bmatrix}$	$\begin{bmatrix}-1/2 & -\sqrt{3}/2\\ -\sqrt{3}/2 & 1/2\end{bmatrix}$

Table 3
Descent of symmetry from symmetry group $\mathbf{C}_{6v}$ to $\mathbf{C}_{3v}$

$\mathbf{C}_{3v}$		$\mathbf{C}_{6v}$
$\{\mathbb{V}^{(A_1)}\}$	$\Leftrightarrow$	$\{\mathbb{V}^{(A_1)}, \mathbb{V}^{(B_1)}\}$
$\{\mathbb{V}^{(A_2)}\}$	$\Leftrightarrow$	$\{\mathbb{V}^{(A_2)}, \mathbb{V}^{(B_2)}\}$
$\{\mathbb{V}^{(E)1}\}$	$\Leftrightarrow$	$\{\mathbb{V}^{(E_1)1}, \mathbb{V}^{(E_2)1}\}$
$\{\mathbb{V}^{(E)2}\}$	$\Leftrightarrow$	$\{\mathbb{V}^{(E_1)2}, \mathbb{V}^{(E_2)2}\}$

$$\tilde{\mathbf{H}} = \begin{bmatrix} \tilde{\mathbf{H}}^{(A_1)} \ (4\times 3) & & & \\ & \tilde{\mathbf{H}}^{(A_2)} \ (2\times 3) & & \\ & & \tilde{\mathbf{H}}^{(E)1} \ (6\times 6) & \\ & & & \tilde{\mathbf{H}}^{(E)2} \ (6\times 6) \end{bmatrix} \quad 12 \tag{21}$$

Each of the equilibrium blocks is of full rank. Obviously, the inextensional mechanism and state of self-stress will be identical to those found in the previous analysis, but the mechanism now occurs in the first equilibrium block $\tilde{\mathbf{H}}^{(A_1)}$, with $\mathbf{C}_{3v}$ symmetry, while the state of self-stress occurs in the second equilibrium block $\tilde{\mathbf{H}}^{(A_2)}$, with 'lesser' $\mathbf{C}_3$ symmetry.

It is the existence of a mechanism, but no state of self-stress, in the first equilibrium block which allows us to show that the mechanism must be finite. In Section 1.2., we noted that an equilibrium matrix with more rows than columns, i.e., a structure with too few constraints, would have a finite mechanism as long as the equilibrium matrix was not rank-deficient. This analysis carries over to the independent equilibrium blocks $\tilde{\mathbf{H}}^{(\mu)i}$, as long as the block-form of the equilibrium matrix is not changed when the mechanism is mobilised. This will be the case if the mechanism is in the first equilibrium block: the block-form depends only on the topology and symmetry of the structure, neither of which is changed by mobilising the mechanism. The finite mechanism is symmetrically distinct from the state of self-stress.

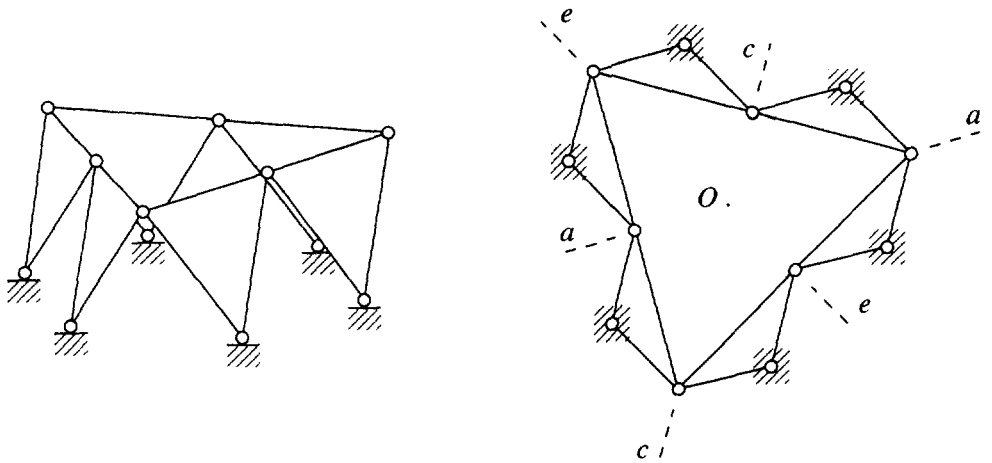

Fig. 8. Hexagonal ring at the bifurcation point, with $\mathbf{C}_{3v}$ symmetry.

Consider a linear displacement of the structure by some finite distance in the direction of the inextensional mechanism. The structure will retain its $\mathbf{C}_{3v}$ symmetry, but because the mechanism will in reality follow a non-linear path, the linear step taken may result in small changes in the length of some bars. However, these extensions must also have $\mathbf{C}_{3v}$ symmetry, and hence can only be corrected by displacements in the $\mathbb{V}_{\mathbf{p}}^{(A_1)}$ subspace. It is impossible for these extensions to have 'lesser' symmetry, e.g., only $\mathbf{C}_3$ symmetry, and hence the state of self-stress, which does have only $\mathbf{C}_3$ symmetry and is therefore situated in symmetry subspace $\mathbb{V}_{\mathbf{f}}^{(A_2)}$, will be unaffected and cannot stiffen the mechanism. Eventually it will be possible to converge on a new configuration along the path of the finite mechanism with the structure retaining its $\mathbf{C}_{3v}$ symmetry.

3. Bifurcation point of the hexagonal ring

In the previous section, we showed that the hexagonal ring's single degree of kinematic indeterminacy represents a finite mechanism with $\mathbf{C}_{3v}$ symmetry. If the mobilisation of a finite mechanism leads to configuration where the degree of kinematic indeterminacy increases, the structure is said to have reached a point of kinematic bifurcation. At such points there exists a multi-dimensional vector space of inextensional mechanisms and there is now a possibility of having a number of distinct kinematic paths that admit finite mechanisms.

If we follow the kinematic path of the finite mechanism in Fig. 6, the hexagonal ring reaches a configuration shown in Fig. 8, which is a point of kinematic bifurcation (Tarnai, 1989). Kumar (1996) analysed the hexagonal ring at the point of kinematic bifurcation using singular value decomposition (SVD) techniques to identify the m inextensional mechanisms and the s states of self-stress. The analysis showed that the equilibrium matrix $\mathbf{H}$ now has rank 15, and hence there now exists $s = 3$ states of self-stress and $m = 3$ inextensional mechanisms. Kumar also showed that in this three-dimensional vector space of inextensional mechanisms there exists four distinct

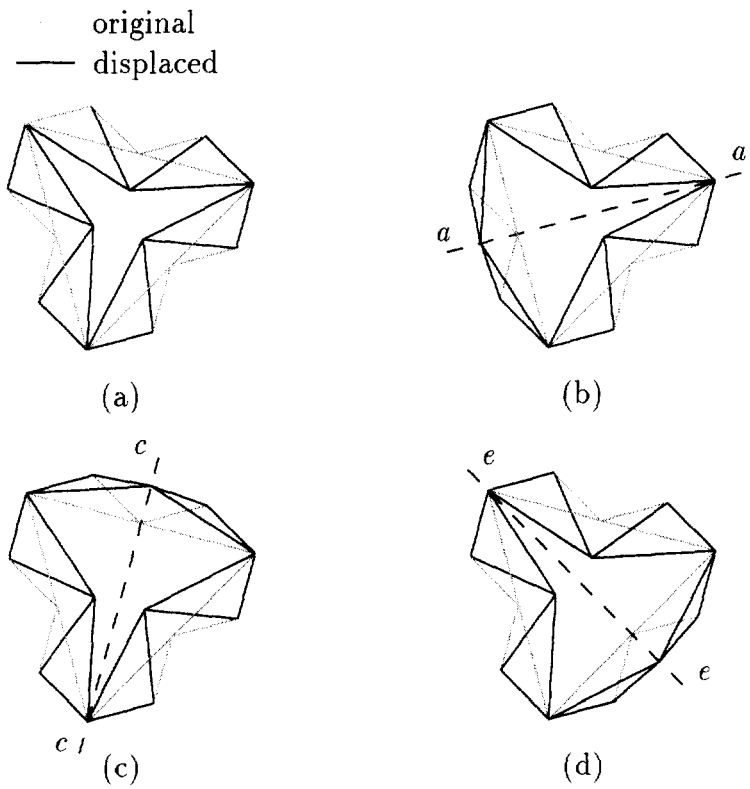

Fig. 9. Finite mechanisms at the bifurcation point.

kinematic paths that admit finite mechanisms, these are shown in Fig. 9. Figure 9(a) shows the original finite mechanism with $\mathbf{C}_{3v}$ symmetry, Fig. 9(b), (c) and (d) show three finite mechanisms which only have reflection symmetry in one of the planes a, c or e.

In this section we will carry out a symmetry analysis to see if we can identify these four finite mechanisms with the hexagonal ring at the point of kinematic bifurcation. Previously, the equilibrium matrix was block-diagonalised using symmetry group $\mathbf{C}_{3v}$, for the hexagonal ring in its original configuration. At the point of kinematic bifurcation the hexagonal ring has $\mathbf{C}_{3v}$ symmetry, and hence the block-diagonalised equilibrium matrix $\tilde{\mathbf{H}}$ will have the same form shown in Eqn 21.

As in Section 2.3., both equilibrium blocks $\tilde{\mathbf{H}}^{(A_1)}$ and $\tilde{\mathbf{H}}^{(A_2)}$ are of full rank. $\tilde{\mathbf{H}}^{(A_1)}$ contains an inextensional mechanism, and $\tilde{\mathbf{H}}^{(A_2)}$ contains a state of self-stress. Now however, the two (6×6) equilibrium blocks $\tilde{\mathbf{H}}^{(E)1}$ and $\tilde{\mathbf{H}}^{(E)2}$, are of rank 5. $\tilde{\mathbf{H}}^{(E)1}$ contains a state of self-stress and an inextensional mechanism which have reflection symmetry in plane a, and $\tilde{\mathbf{H}}^{(E)2}$ contains a state of self-stress and an inextensional mechanism which have reflection anti-symmetry in plane a.

From the symmetry analysis it is clear that the original finite mechanism remains in the submatrix block $\tilde{\mathbf{H}}^{(A_1)}$ and hence is not stabilised by any states of self-stress. Now however, we will try to identify the remaining three finite mechanisms that exist in the 3-dimensional vector space of

Table 4
Irreducible representations of symmetry group $\mathbf{C}_s$

$\mathbf{C}_s$	E	σ_a
$\Gamma^{(A_1)}$	1	1
$\Gamma^{(A_2)}$	1	−1

inextensional mechanisms. Kumar's analysis showed that the remaining three finite mechanisms have only reflection symmetry in one of the planes a, c or e. We can choose the following two symmetry operations to constitute the symmetry group $\mathbf{C}_s$:

(1) The identity, symmetry operation E.
(2) Reflection in the vertical plane a, symmetry operation σ_a.

The load vector space $\mathbb{V}_\mathbf{p}$ and the bar-force vector space $\mathbb{V}_\mathbf{f}$ are each decomposed into two symmetry subspaces, defined by the irreducible representations of symmetry group $\mathbf{C}_s$, shown in Table 4. The symmetry subspaces $\mathbb{V}_\mathbf{p}^{(A_1)}$ and $\mathbb{V}_\mathbf{f}^{(A_1)}$ have reflection symmetry in plane a, while the symmetry subspaces $\mathbb{V}_\mathbf{p}^{(A_2)}$ and $\mathbb{V}_\mathbf{f}^{(A_2)}$ have reflection anti-symmetry in plane a.

Again, it is not necessary to completely reanalyse the structure using symmetry group $\mathbf{C}_s$, Table 5 shows how the $\mathbf{C}_{3v}$ symmetry subspaces combine to form the $\mathbf{C}_s$ symmetry subspaces. Using the load and bar-force vector symmetry-adapted coordinate systems with $\mathbf{C}_s$ symmetry properties, the block diagonalised matrix $\tilde{\mathbf{H}}$ now has the form shown in Eqn. 22.
The equilibrium block $\tilde{\mathbf{H}}^{(A_1)}$ is of rank 8 and hence contains a 2-dimensional vector space of inextensional mechanisms and a single state of self-stress, all with reflection symmetry in plane a. The equilibrium block $\tilde{\mathbf{H}}^{(A_2)}$ is of rank 7 and hence contains a single inextensional mechanism and a 2-dimensional vector space of self-stress, all with reflection anti-symmetry in plane a.

In contrast with Section 2, symmetry subspace $\mathbb{V}_\mathbf{f}^{(A_1)}$ contains a single state of self-stress. Thus, displacing the structure by some finite combination of the two linear mechanisms in symmetry subspace $\mathbb{V}_\mathbf{p}^{(A_1)}$, will cause bar-extensions which have reflection symmetry in plane a. Now however, there is a potential internal geometric incompatibility associated with this step, indicated by the existence of a state of self-stress with the same symmetry. The state of self-stress may ensure that

Table 5
Descent of symmetry from symmetry group $\mathbf{C}_{3v}$ to $\mathbf{C}_s$

$\mathbf{C}_s$		$\mathbf{C}_{3v}$
$\{\mathbb{V}^{(A_1)}\}$	$\Leftrightarrow$	$\{\mathbb{V}^{(A_1)}, \mathbb{V}^{(E)1}\}$
$\{\mathbb{V}^{(A_2)}\}$	$\Leftrightarrow$	$\{\mathbb{V}^{(A_2)}, \mathbb{V}^{(E)2}\}$

$$\tilde{\mathbf{H}} = \begin{bmatrix} \tilde{\mathbf{H}}^{(A_1)} \\ (10\times 9) & \\ & \tilde{\mathbf{H}}^{(A_2)} \\ & (8\times 9) \end{bmatrix} \tag{22}$$

the only way of correcting these extensions is for the structure to return to its original configuration, thus showing that the combination chosen may not be a finite path.

A way forward appears to be possible because we have already found one of the finite mechanisms. The descent of symmetry from $\mathbf{C}_{3v}$ to $\mathbf{C}_s$ clearly shows that the original finite mechanism shown in Fig. 9(a), is again in the first symmetry subspace $\mathbb{V}_{\mathbf{p}}^{(A_1)}$. From Kumar's analysis we already know the symmetry properties of the three remaining finite mechanisms and hence the finite mechanism with reflection symmetry in plane a, shown in Fig. 9(b), must also be contained in $\mathbb{V}_{\mathbf{p}}^{(A_1)}$. However, these two finite mechanisms are, in fact, not orthogonal, and so this does not help us to find the second finite path. In this case, finding the other finite paths requires a non-linear analysis.

The remaining two finite mechanisms with reflection symmetry in planes c and e, shown in Fig. 9(c) and 9(d) respectively, are not contained in either $\mathbb{V}_{\mathbf{p}}^{(A_1)}$ or $\mathbb{V}_{\mathbf{p}}^{(A_2)}$. To find symmetry subspaces which contain these finite mechanisms, we must choose the symmetry operations $\{E, \sigma_c\}$ or $\{E, \sigma_e\}$ to constitute the symmetry group $\mathbf{C}_s$. We would then find that the symmetry subspace $\mathbb{V}_{\mathbf{p}}^{(A_1)}$ has reflection symmetry in plane c or e, and hence contain the corresponding finite mechanism.

It should be noted that the $\mathbf{C}_{3v}$ and $\mathbf{C}_s$ symmetry subspaces have combined in this way due to the particular choice of 2-dimensional irreducible representation $\Gamma^{(E)}$, of symmetry group $\mathbf{C}_{3v}$. As explained in Kangwai et al. (1999), 2-dimensional irreducible representations are not unique (although 1-dimensional irreducible representations are). A different choice could have resulted in symmetry subspaces $\mathbb{V}^{(E)1}$ and $\mathbb{V}^{(E)2}$ having reflection symmetry and anti-symmetry in plane c or e.

4. Comments on the identification of finite mechanisms

Section 2 has shown that, for some special statically and kinematically indeterminate structures, the identification of a finite mechanism is possible based only on a linear analysis, along with symmetry arguments. However, Section 3 has shown that such an analysis cannot always identify all the finite mechanisms in such a structure. This section will identify the conditions under which a finite mechanism can be identified.

The argument put forward in Section 2 for the existence of a finite mechanism is valid when a mechanism exists in symmetry subspace $\mathbb{V}_{\mathbf{p}}^{(A_1)}$, and no states of self-stress exist in the corresponding symmetry subspace $\mathbb{V}_{\mathbf{f}}^{(A_1)}$, i.e., any states of self-stress have 'lesser' symmetry properties. In this

case, the state of self-stress is always independent of the mechanism and hence can never prevent its motion. The same argument is equally valid for n mechanisms in symmetry subspace $\mathbb{V}_{\mathbf{p}}^{(A_1)}$, as long as there are no states of self-stress in symmetry subspace $\mathbb{V}_{\mathbf{f}}^{(A_1)}$. Then these n mechanisms define an n-dimensional space of possible finite mechanisms.

It should be noted that the symmetry analysis does not have to utilise the full symmetry of the structure. Instead, the analysis should be carried out using the symmetry of a mechanism. If this shows that all the states of self-stress in the structure have 'lesser' symmetry, then this mechanism will be finite. As shown in Sections 2 and 3, this analysis can be based on the descent of symmetry, and hence a full reanalysis of the structure is not required.

By contrast, Section 3 has shown it is not possible to find *all* the finite mechanisms using a symmetry analysis. If a state of self-stress exists in symmetry subspace $\mathbb{V}_{\mathbf{f}}^{(A_1)}$, then for any particular combination of the inextensional mechanisms in $\mathbb{V}_{\mathbf{p}}^{(A_1)}$, it is not possible to say whether the mechanism would be stiffened by this state of self-stress. In this case, a non-linear analysis is required to find the finite mechanism.

It should be pointed out that, of course, the current analysis is only completely valid for perfect structures. Thus, for example, a full analysis of a slightly imperfect ring structure may find it is *not* rank deficient, and is theoretically *not* a mechanism. Despite this, our analysis remains valid. A simple (inevitably imperfect) model of the ring structure *does* show the finite mechanism behaviour predicted, with no noticeable resistance to motion beyond that required to flex hinges. Indeed the same behaviour has been observed in models of a number of other similar structures analysed by Kangwai (1997). A small amount of flexibility is all that is required for the structure to escape the effect of the imperfection.

In conclusion, this paper has shown that, if an analysis is carried out using the symmetry of an inextensional mechanism, and any states of self-stress in the structure have some 'lesser' symmetry properties, then this mechanism will be finite.

References

Altmann, S.L., Herzig, P., 1994. Point-Group Theory Tables. Clarendon Press, Oxford.

Calladine, C.R., 1978. Buckminster Fuller's 'Tensegrity' structures and Clerk Maxwell's rules for the construction of stiff frames. Int. J. Solids Structures 14, 161–172.

Föppl, A., 1912. Vorlesungen über Technische Mechanik. Vol. 2. Teubner, Leipzig and Berlin.

Fuller, R.B., 1975. Synergetics: Explorations in the Geometry of Thinking. Macmillan Publishing Co., New York.

Kangwai, R.D., 1997. The analysis of symmetric structures using group representation theory. PhD thesis, University of Cambridge.

Kangwai, R.D., Guest, S.D., Pellegrino, S., 1999. An introduction to the analysis of symmetrical structures. Computers and Structures 71, 671–688.

Kangwai, R.D., Guest, S.D., 1999. Symmetry-adapted equilibrium matrices. Int. J. Solids Structures, in press.

Kötter, E., 1912. Über die Möglichkeit, n Puckte in der Ebene oder im Raume durch weinger als $2n$-3 oder $3n$-6 Stäbe von ganz unveränderlicher Länge unverschieblich miteinander zu verbinden. In Festschrift Heinrich Muller-Breslau. Kröner, Leipzig, pp. 61–80. Cited by Pellegrino and Calladine (1991).

Kumar, P., 1996. Kinematic Bifurcations and Deployment Simulations of Foldable Space Structures. PhD Thesis, University of Cambridge.

Kuznetsov, E.N., 1988. Underconstrained structural systems. Int. J. Solids Structures 24, 153–163.

Kuznetsov, E.N., 1991. Systems with infinitesimal mobility. J. Appl. Mech. 58, 513–526.

Maxwell, J.C., 1864. On the calculation of the equilibrium and stiffness of frames, Phil. Mag. 27 (4th series), 294–299. Reprinted in Niven, W.D. (1890). The Scientific Papers of J.C. Maxwell, Vol. 1, Cambridge University Press, Cambridge, pp. 598–604.

McGuire and Gallagher, 1979. Matrix Structural Analysis. John Wiley & Sons.

Mohr, O., 1885. Beitrag zur Theorie des Fachwerkes. Der Civilgenieur 31, 289–310. Cited by Pellegrino and Calladine (1991).

Pellegrino, S., Calladine, C.R., 1986. Matrix analysis of statically and kinematically indeterminate frameworks. Int. J. Solids Structures 22, 409–428.

Pellegrino, S., Calladine, C.R., 1991. First-order infinitesimal mechanisms. Int. J. Solids Structures 27, 505–515.

Tarnai, T., 1980. Simultaneous static and kinematic indeterminacy of space trusses with cyclic symmetry. Int. J. Solids Structures 16, 347–359.

Tarnai, T., 1989. Finite mechanisms and the timber octagon of Ely Cathedral. Structural Topology 14, 9–20.